Food Safety and Risk

RESEARCH

Open Access

Evaluation of the performance of Nanoparticle Tracking Analysis (NTA) for the measurement of nanoplastics

Ruud J. B. Peters[2], Emma Relou[1], Eelco L. E. Sijtsma[1] and Anna K. Undas[1*]

Abstract

In recent years, microplastics have been detected in fresh- and seawater, the atmosphere, sediments, soils, sewage sludge, biota, and food. However, these microplastics can degrade into even smaller plastic particles in the submicron range, referred to as nanoplastics. Due to their smaller dimensions and colloidal properties, nanoplastics could pose an increased hazard to the environment, biota and humans. While there are methods for detecting microplastics, the reliable detection and quantification of size and particle number concentrations of plastic particles less than a micrometre in size are still difficult. In this study, we describe the development and validation of a method for detecting nanoplastics using nanoparticle tracking analysis (NTA) and discuss the limitations of the method in the analysis of nanoplastics. Our method proved accurate and precise for 102 nm polystyrene Nanospheres, with a linear concentration ranging from 5.0×10^6 to 2.0×10^9 particles/mL, and a particle size range from 46 to over 350 nm. However, several limitations of the NTA method became apparent. When measuring polydisperse particle mixtures, NTA tends to underestimate the presence of smaller particles due to lower scattering intensity and overlapping signals. Moreover, NTA cannot chemically discriminate between nanoplastics and other types of nanoparticles, such as natural organic matter, leading to potential overestimation of plastic particle concentrations. Despite these weaknesses, the validated method was applied to eight brands of bottled mineral water. We detected particles with mean particle sizes in the range of 110 to 170 nm, and particle number concentrations between 1.0×10^6 to 2.2×10^7 particles/mL. Particle size distributions showed a particle size range of 50 to 500 nm. However, due to the limitations of NTA, it was not possible to conclusively confirm that the detected particles were nanoplastics, and therefore, the reported concentrations refer to the total particle content rather than specifically to nanoplastics.

Keywords Nano tracking analysis (NTA), Nanoplastics detection, Bottled mineral water, Method optimisation and validation

Introduction

Microplastics (MPs) refer to small, microscopic solid polymer particles with sizes <5 mm. Until recently (European Commission, 2023), MPs could be intentionally added to consumer products (primary MPs), but more often they are unintentionally generated by the degradation of bulk plastic litter (secondary MPs). Once released or generated by litter degradation, they are associated with long-term environmental persistence and are regarded as emerging contaminants. In the last few

*Correspondence:
Anna K. Undas
anna.undas@wur.nl
[1] Wageningen Food Safety Research (WFSR), Part of Wageningen University & Research, Akkermaalsbos 2, Wageningen 6708 WB, The Netherlands
[2] Saxion University of Applied Sciences, Lectorate Technologies for Criminal Investigations, Handelskade 75, Deventer 7417 DH, The Netherlands

years, MPs have been detected in fresh- and seawater, atmosphere, sediments, soils, sewage sludge, biota and food (Bouwmeester et al., 2015; Alexy et al. 2020; Barbosa et al., 2020; van Raamsdonk et al., 2020; Zhang et al., 2020; Vitali et al., 2022). However, these MPs can degrade to even smaller plastic particles in the sub-micron range, the nanoplastics (NPs). There is still some debate about the definition of the term NPs, with some authors suggesting particles smaller than 100 nm (Koelmans et al. 2015; Hernandez et al., 2017), while others suggest smaller than 1000 nm (ISO/TR 21960:2020; Hartmann et al., 2019; Frias and Nash (2019). In the present study, we define NP as plastic particles in the size range of 1 to 1000 nm.

The presence of NPs was detected in seawater and only very recently in soil (Ter Halle et al., 2017; Wahl et al., 2021). However, only a few studies have confirmed NPs' presence in other environmental samples (Materić et al., 2020; Cai et al., 2021). In addition, several studies have investigated the possibility of plastic debris fragmenting into nano-sized plastic particles by UV radiation (Lambert and Wagner, 2016a), mechanical energy (Ekvall et al., 2019) and by digestive fragmentation (Dawson et al., 2018). Furthermore, NPs have been demonstrated to be released using personal care products (Hernandez et al., 2017), boiling plastic teabags (Hernandez et al., 2019), and using plastic infant bottles (Li et al., 2020). Due to their smaller dimensions and colloidal properties, NPs could pose an increased hazard to the environment, biota and humans (Moiniafshari et al., 2025). Currently, the risks associated with accidental exposure to humans and wildlife is raising concern among the general public and awareness of the regulatory authorities (Kiran et al., 2022; Singh et al., 2022; Lai et al., 2022; Gruber et al., 2022).

While there are methods of detecting microplastics, the reliable detection and quantification of size and particle number concentrations of plastic particles less than a micrometre in size is still difficult (Caputo et al., 2021). Currently, there is no method available that is inexpensive, builds on existing techniques and can be automated for high-throughput analysis of nanoplastic particle suspensions. Both dynamic light scattering (DLS) and nanoparticle tracking analysis (NTA) are suitable methods to determine the particle size distribution in aqueous suspension. DLS and NTA are complementary techniques; they depend on Brownian motion and light scattering and apply the Einstein-Stokes equation. However, there is also a difference: DLS is an intensity-based method that requires high concentrations, or particles with high scattering cross-sections, while NTA is number-based because of its particle-by-particle analysis. NTA can access lower particle concentrations and give better results for polydisperse samples (Kestens et al., 2017). According to Roesch et al. (2022), NTA also gives a better resolution between different particle sizes and more accurate quantification of particle concentrations. Considering the abovementioned aspects, NTA poses a better technique for analysing MPs or NPs. Still, despite their advantages over DLS, both techniques can only determine the total particle concentration and their hydrodynamic sizes, and are unable to chemically distinguish the types of detected polymers, nor differentiate between plastic particles, organic matter, or other scattering particles. Nevertheless, NTA, despite its limitations, may be a suitable method for characterizing particles in validation and standardization studies where the chemical composition of the analyzed polymers is known.

NTA consists of three steps: particle(s) visualisation, recording particle movement and processing the recorded video. Particle visualisation is achieved by directing a laser beam at the particles that scatter the laser beam's light. The camera level adjusts the brightness of the view. Recording the Brownian motion of the particles is generally done with a capturing time of 60 s. After recording, the Brownian motion of the particles is tracked by analysing the shift of a particle's centre between two video frames. Setting the detection threshold, particles are included or excluded based on a minimum value of light scattering intensity. Particle movement can then be used to estimate the particle size. The particle concentration can be assessed by counting the number of tracked particles.

Only a limited number of studies focus on applying NTA to analyse nano- and microplastics. Lambert and Wagner (2016a) applied NTA to prove the degradation of polystyrene disposable coffee cup lids. This study was part of another study where NTA was applied to indicate the formation of particles in the range of 30–2000 nm due to the degradation of different polymers (Lambert and Wagner, 2016b). Oelschlägel et al. (2018) investigated the weathering of microplastics in the marine environment by imitating these conditions and applying NTA for the analysis of particles smaller than 1.2 μm. These limited studies show that NTA can be applied to small MPs and NPs. Our study aims to develop a method for determining particle size distributions in bottled water using NTA. To achieve this, the research is based on three building blocks: NTA analytical optimization for polystyrene nanoparticles (NPLs), determining the performance characteristics of NTA for polystyrene NPLs analysis, and the sample preparation of bottled water. The goal of this study is to provide an easy-to-follow protocol that outlines all steps necessary for method validation for the analysis of polystyrene NPLs using NTA. In the final step of the study, the developed method is applied to a real-world scenario in which bottled drinking water is analyzed for the presence of particles in the nanometer size range, which, due to the limitations of the method, can not be concluded to be nanoplastics (NPs).

Methods and materials

Chemicals

Chemicals used in this study were ethanol (Emsure grade, Merck, Germany), mainly for instrument cleaning, and MilliQ water generated by a MilliPore system (MilliPore, USA) for the preparation of suspensions and blank control samples. Sodium dodecyl sulphate (Acros Organics, Belgium) and Triton X-100 (BioXtra grade, Sigma, USA) were used to prepare stable particle suspensions. The particle standards used were 3000 series polystyrene (PS) nanospheres, 1% solids, with certified sizes (mean diameters) determined by TEM: 350 ± 6 nm, 203 ± 5 nm, 102 ± 3 nm, 46 ± 2 nm, 40 ± 1 nm and 30 ± 1 nm (Thermo Fisher Scientific, USA).

Cans (500 mL) with purified compressed air to clean and blow dry instrument surfaces were from Dataflash (Germany) and Kontakt Chemie (Belgium).

Samples

Samples used in this study were still mineral water in single-use plastic bottles from eight different brands obtained from one single retail shop in the Netherlands (later abbreviated A-H). The volumes of these bottles ranged from 500 to 750 mL.

Instrumentation

The analytical instrument used in this study was a NanoSight NS300 obtained from Malvern Panalytical (UK), equipped with a 405 nm laser module, an O-ring top-plate and a low flow-cell top-plate. The low flow-cell top-plate was combined with a NanoSight syringe pump obtained from Malvern Panalytical (UK). The data were processed using NTA software version 3.4 (Build 3.4.003). The NTA method for NPs was developed by optimising the camera level, capturing the time and detection threshold of the NanoSight NS300 (NS300). Optimal detection parameters were selected and used to determine the performance characteristics. The NS300 allows for working with different measuring cells: the O-ring top-plate or a low flow-cell top-plate, which is applicable in both flow and static mode. These three instrument modes were compared by assessing their repeatability, within-laboratory reproducibility and accuracy.

In the default method, the low flow-cell top-plate was used. Before insertion of the sample into the cell, the syringe was rinsed with 0.5 mL sample and checked for air bubbles. The measuring cell was then rinsed with 3 mL MilliQ water and 0.5 mL sample. Once the sample was inserted, the image position was adjusted till the laser beam was centred in the field of view. Shutter and camera gain were set to automatic. Focus and camera levels were set with auto-setup and checked manually. Each sample was recorded five-fold with a capturing time of 60 s and a flow speed of 50 a.u. The experiments described in this paper were performed in a temperature-controlled laboratory, with the temperature maintained at 20 °C. During analysis, the NS300 temperature sensor was not used (set to the "off" setting), and the temperature was manually set to 20 °C. At this temperature, the dynamic viscosity of water is 1 mPa·s. Since the samples were prepared in MilliQ water, this viscosity value was used as the input parameter in the NS300 software. After analysis, the videos were processed. Blur, minimum expected particle size and minimum track length were set to automatic. The detection threshold was adjusted until most particles were marked with a red cross, and no more than five blue crosses (i.e. noise) were visible per frame. The size distribution graphs were obtained by the NTA software via the "finite track-length adjusted" (FTLA) algorithm.

Results and discussion

Camera level (CL) and detection threshold (DT) optimisation

At first, the PS nanoparticles detection with the NS300 using different camera levels (CL) and detection thresholds (DT) settings was optimised. To do so, an aqueous suspension of 102 nm Nanospheres with a particle concentration of 4.0×10^8 particles/mL was prepared, analysed with varying CL settings (9–14), and processed with three different DT settings (5, 10, 15). The influence of both parameters on the particle concentration is illustrated in Fig. 1.

Figure 1 shows no strong overall correlation between CL and DT and particle concentration; however, significant differences were observed for CL levels 12 and 14. A slight underestimation of the particle concentration is generally seen with CL levels 10 and 11. Notably, from CL 11 and up, the particle concentration increases with camera level. Based on the particle'suspensions'pre paration, it was expected that the particle concentration should be within the range of 80–110% of the prepared value, and that is indeed the case for all CL and DT levels, except for the settings CL 13 and 14 with DT 5 where the particle concentration is slightly overestimated. Therefore, CL 12 with DT of 5 or 10 were selected as the most optimum settings giving the closest to the prepared particle concentration value with the lower standard deviation (SD) in the determined particle concentration.

The influence of CL and DT on both the mean and mode hydrodynamic particle size was also determined using the 102 nm Nanospheres. The reference value for

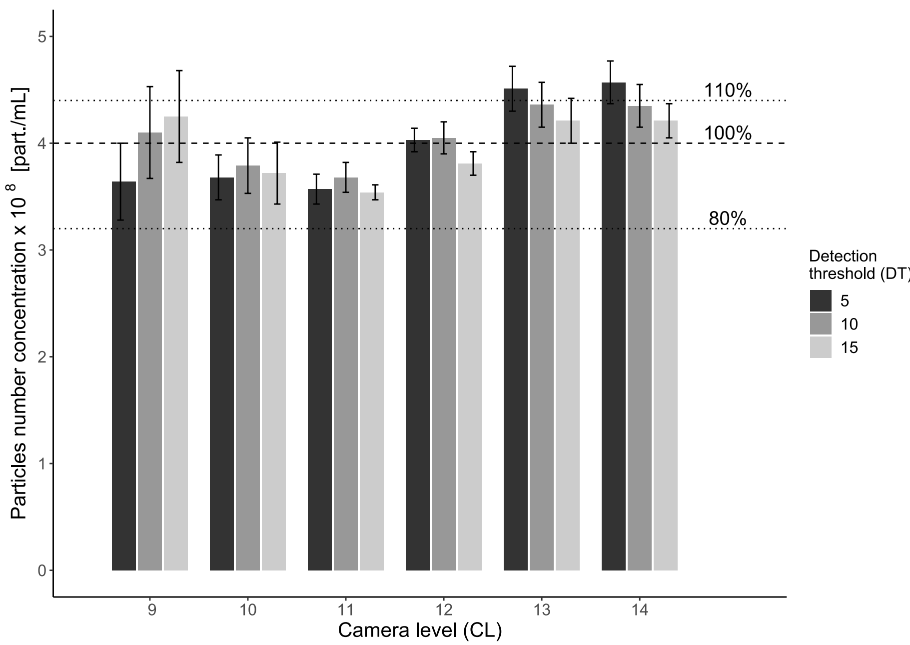

Fig. 1 The influence of camera levels (CL) and detection thresholds (DT) on the particle concentration expressed in particles/mL as determined for an aqueous suspension of 102 nm Nanospheres with a particle concentration of 4.0×10^8 particles/mL. Bars indicate ± 1 standard deviation

the particle size of this particle, determined by TEM, was 102 ±3 nm. The mean particle size provides information about the average particle size, while the mode particle size provides information about the most common particle size. The results for the different CL and DT settings are presented in Figs. 2 and 3.

Unlike concentration, particle size is affected by CL settings. Both Figs. 2 and 3 show a decreasing particle size with increasing CL. Higher CL leads to more

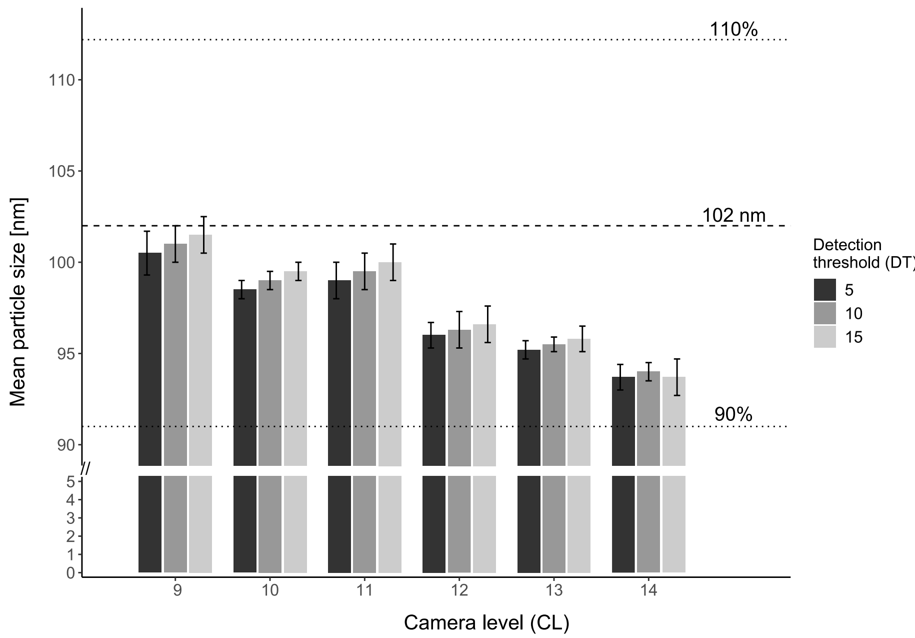

Fig. 2 The influence of the camera levels (CL) and detection thresholds (DT) on mean particle size expressed in nm as determined for an aqueous suspension of 102 nm Nanospheres. Bars indicate ± 1 standard deviation

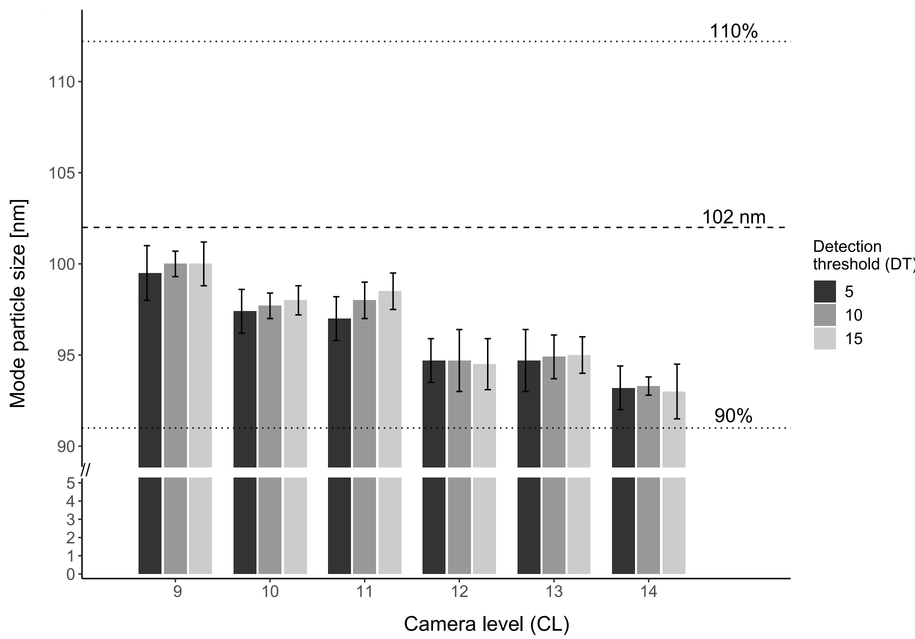

Fig. 3 The influence of the camera levels (CL) and detection thresholds (DT) on mode particle size expressed in nm as determined for an aqueous suspension of 102 nm Nanospheres. Bars indicate ± 1 standard deviation

exposure to the light scattering of the particles, making it more difficult for the processing software to locate the particle centre and track the particle motion. In practice, the determined particle size was expected to be within 90–110% of the reference value of the particle, which means that all particle sizes between 92 and 112 nm would be acceptable. While CL 9 best agrees with the reference value, CL 10 gives a lower SD for both mean and mode particle size. In Figs. 2 and 3, one can also observe that a higher DT gives a larger particle size; however, this impact is insignificant since the impact is generally more negligible than the SD. Based on the particle concentration and size measurements, the optimal settings for further experiments were chosen as CL 11 in combination with DT 15.

Capturing time (CT) optimisation

The capturing time (CT) may also influence the results. Therefore, the 102 nm Nanosphere suspension with a particle concentration of 4.0×10^8 particle/mL was also analysed with capturing times of 30, 60 and 120 s to optimise this parameter. The effect of the capturing time on the determined particle concentration is presented in Fig. 4.

Figure 4 shows an increase in accuracy and precision with increasing capturing time. The increase in precision results from longer capturing time due to a higher analysis volume. Figure 5 overviews the influence of increasing capturing time on both the mean and the median particle size. The precision of the mean particle size decreases with increasing capturing time, with no significant impact on the accuracy. The precision of the mode particle size was highest at a capturing time of 60 s. Somewhat surprisingly, the accuracy of the mode particle size increased with a longer capture time. Regarding both particle size and concentration, a capturing time of 60 s was selected for further experiments as a compromise between precision and accuracy.

Sample flow optimisation

As the last parameter, the influence of the sample flow in the flow cell was determined with the flow speed varying between 25, 50 and 75 a.u. Figure 6 shows the influence of the flow speed on the determined particle concentration. Results show that the most accurate concentration is found at a flow speed of 50 a.u. At the time, the precision is best at a flow speed of 75 a.u. This is expected since a higher flow speed increases the total analysed sample volume; however, a too high flow speed makes it harder for the processing software to track the particle motion, which could decrease the number of tracked particles.

An overview of the influence of flow speed on particle size is given in Fig. 7. The impact of flow speed is relatively small and shows no correlation to the particle size in both mean and mode size. For the mean size, the highest accuracy is found at a flow speed of 25 a.u., while

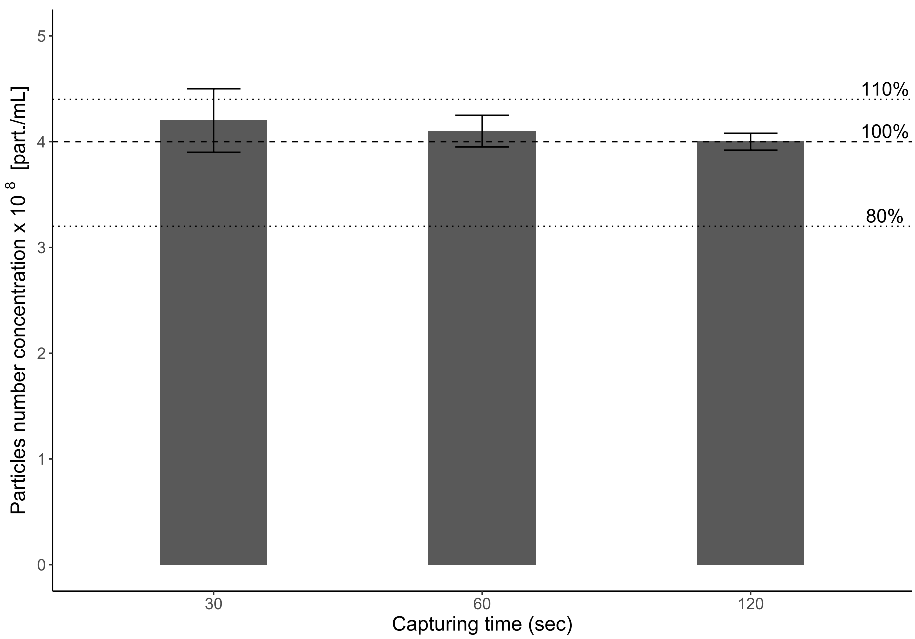

Fig. 4 The influence of capturing time on particle concentration expressed in particles/mL as determined for an aqueous suspension of 102 nm Nanospheres with a particle concentration of 4.0×10^8 particles/mL was analysed five-fold with CL 11 and DT 15. Bars indicate ± 1 standard deviation

for mode size, the highest accuracy was found at a flow speed of 50 a.u. The precision was highest at a flow speed of 75 a.u. for mean particle size and 50 a.u. for mode particle size.

The tested flow speeds have only a minor influence on particle concentration and size. There is no clear correlation between accuracy and precision. A flow speed of 50 a.u. was chosen as optimal because of sample volume reduction compared to a flow of 75 a.u.

Analytical method validation characteristics

Now that the different parameters are optimised, the performance characteristics of the entire method were determined at particle concentrations of 4.0×10^8 and 2.0×10^7 particles/mL using the same 102 nm Nanospheres. The accuracy, repeatability (RSD_r) and within-laboratory reproducibility (RSD_{RL}) were determined using the low flow-cell top-plate and the O-ring top-plate (no flow). To determine repeatability, measurements were carried out in seven-fold in one day. To determine within-laboratory reproducibility, these measurements were repeated on two more days, totalling three days. One-way ANOVA was performed to determine the accuracy, RSD_r and RSD_{RL}, and the results are presented in Table 1.

At the higher particle concentration, the NS300 NTA instrument shows reliable results for the analysis of 102 nm Nanospheres. The accuracy of the particle concentration is well within the expected 80–110% range, while the results for particle size are well within the 90–110% range. Except for the accuracy, the low flow-cell and the O-ring top-plate results are comparable, with those using the O-ring top-plate slightly better. At the lower particle concentration, it is clear that the low particle count influences repeatability and within-laboratory reproducibility. Except for the accuracy of particle concentration measured with the O-ring top-plate, the results for the accuracy are within the expected range. In this case, the configuration with the O-ring top-plate is overestimating the particle concentrations. It is also visible that the repeatability and within-laboratory reproducibility are higher with the O-ring top-plate than with the low flow-cell top-plate. While the differences between the low flow-cell and O-ring top-plate were minimal at the higher particle concentration, the results at the lower particle concentration seem to suggest that using the low flow-cell is beneficial at low particle concentrations. Therefore, the low flow-cell configuration was used in most experiments.

In order to determine the working range for particle size, a calibration curve with particle sizes ranging from 30 to 350 nm was established. The calibration curves of both the mean and mode particle size are presented in Fig. 8. This figure represents a five-fold analysis of each standard, with on the x-axis the reference value and on the y-axis the determined particle size. Both calibration curves met the criterion of $R^2 > 0.99$, indicating linearity.

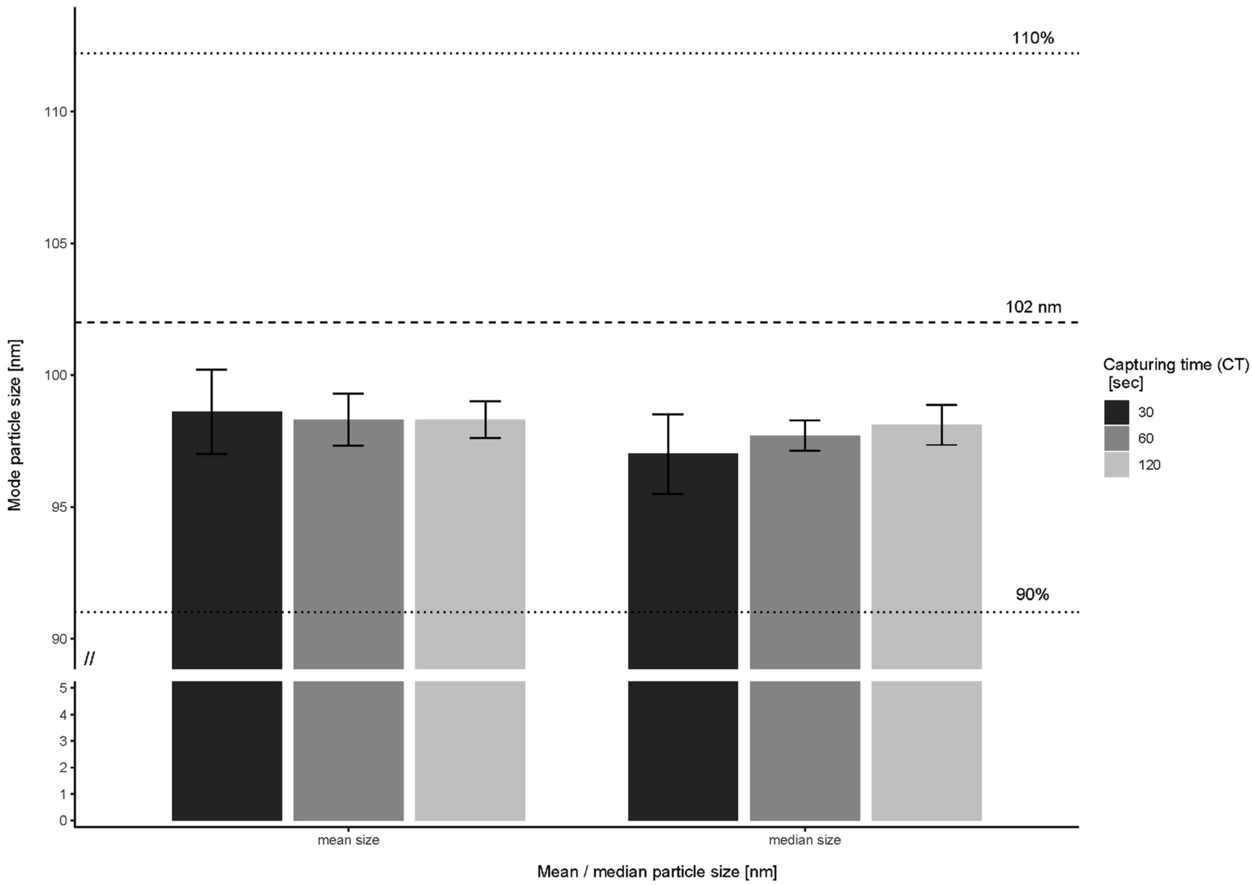

Fig. 5 The influence of the capturing times (CT) on mean and median particle size expressed in nm as determined for an aqueous suspension of 102 nm Nanospheres analysed five-fold using CL 11 and DT 15. Bars indicate ± 1 SD

The accuracy and repeatability for the mean and mode particle size of each calibration point are also given in Table 2. If the accuracy of 90–110% is used as the criterion for the working range for particle size of the NS300, then the lower limit of particle size detection is 46 nm. The upper limit of particle size is > 350 nm, and with the technique of NTA, the particle size determination is limited to the nano-range, i.e. < 1000 nm. Recently, Caputo et al. (2021) have determined this for various techniques and gave an upper limit of 800 nm for NTA.

In order to determine the working range for particle concentration, a calibration curve with particle concentrations ranging from 5.0 $\times 10^6$ to 2.0 $\times 10^9$ particles/mL was prepared. The calibration curve is presented in Fig. 9, again as a five-fold analysis for each standard. The x-axis shows the reference value, and on the y-axis, particle concentration is determined. The calibration curve meets the criterion of $R^2 > 0.99$, meaning the response is linear in the calibration range. The accuracy and repeatability of the particle concentration are given in Table 3. The working range criterion for particle concentration is an accuracy of 80–110%, and a maximum repeatability according to the Horwitz equation (RSD_r max $= 2\ C^{-0.15}$ where C is expressed as an exponent of 10). From this, it can be concluded that the working range for the particle concentration ranges from 1.0×10^7 to 2.0×10^9 part./mL.

To test if NTA can distinguish between different particle sizes in the same sample, i.e. analyse polydisperse samples, three different mixtures with two particle sizes were analysed: a mixture of 46 and 102 nm particles, a mixture of 102 and 203 nm particles, and a mixture of 46 and 203 nm particles. In all mixtures, the particle number concentration of the two types of particles was equal and about 1.0×10^8 particles/mL. All mixtures were analysed five-fold, and the results are expressed as accuracy and relative standard deviation in Table 4.

While the accuracy and particle size of the larger particles in a mixture are as expected, the particle number concentrations of the smaller particles in a mixture are largely underestimated. The particle size of the smaller particles in a mixture is as expected, at least if these

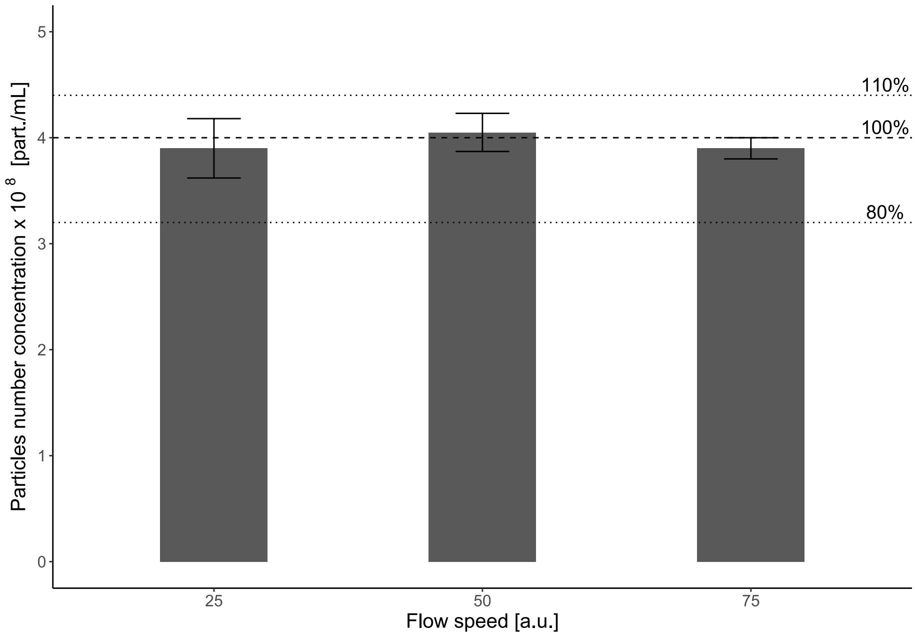

Fig. 6 The influence of flow speed on the particle concentration expressed as particles/mL as determined for an aqueous suspension of 102 nm Nanospheres with a particle concentration of 4.0×10^8 particles/mL analysed five-fold with CL 11 and DT 15 and with a capturing time of 60 s. Bars indicate ± 1 standard deviation

particles are observed. The reason for these differences is that large particles scatter light much more strongly than small particles. The intensity of the scattered light relates to the particle size to the power of six. In the mixture of 46 and 203 nm particles, the 203 nm particle scatters light 4.4^6 (= 7400) times more strongly than the 46 nm particle. Consequently, in the mixture, the 46 nm particle, a particle size already on the limit of detection, is virtually invisible and undetected. In the mixture of 46 and 102 nm particles, we can only observe the 46 nm particles. In the case of the mixture of the 102 and 203 nm particles, both particles are well observed, but the concentration of the smaller-sized particle is still underestimated by a factor of 2. In real samples, this is a serious problem since the particle numbers of small particles may be strongly underestimated when large particles are present.

Analysis of bottled water samples

Finally, the validated method was used to determine the presence of nanosized particles in bottled water. It was expected that the concentration of particles in bottled water was low. Therefore, it was decided to use the maximum video capturing time of 180 s to count more particles and thus lower the linear range of the particle number concentration. In addition, it was expected that there might be largesignificant differences between the particle content in individual bottles of the same brand. Therefore, ten individual bottles were analysed from each brand. It was also assumed that all particles detected by NTA were of plastic origin, although this cannot be confirmed using this technique. Particle sizes were calculated assuming the particles were spherical and had a density of 1 g/cm^3. In total, eight brands of mineral bottled water samples (A-H) were analysed. After opening each bottle, a subsample was collected and measured with the NTA instrument directly without any sample processing. The results of the particle number concentration and average particle size (mean and mode) are given in Table 5. Generally, the particle number concentration is between 1.0 $\times 10^6$ and 4.0 $\times 10^6$ particles/mL, which is actually on the verge of the lower limit of the linear concentration range, taking into account the longer video capturing time. Two samples did show higher particle number concentrations of 1.5×10^7 (A) and 2.2×10^7 (E) particles/mL, and are clearly within the linear concentration range of the NS300. For the other samples the concentration values are indicative since the repeatability at those low concentrations is probably higher.

Considering particle sizes, the mass-based particle concentrations are in the range of 0.01 to 0.06 mg/L (ppm). The relative standard deviation (RSD in Table 5) reflects not only the reproducibility (in the validation 37% at a particle number concentration of 2.0×10^7) but also the difference in particle content in the ten different bottles from one brand. This is particularly clear from brand A where we found an RSD_{RL} of 165%, indicating

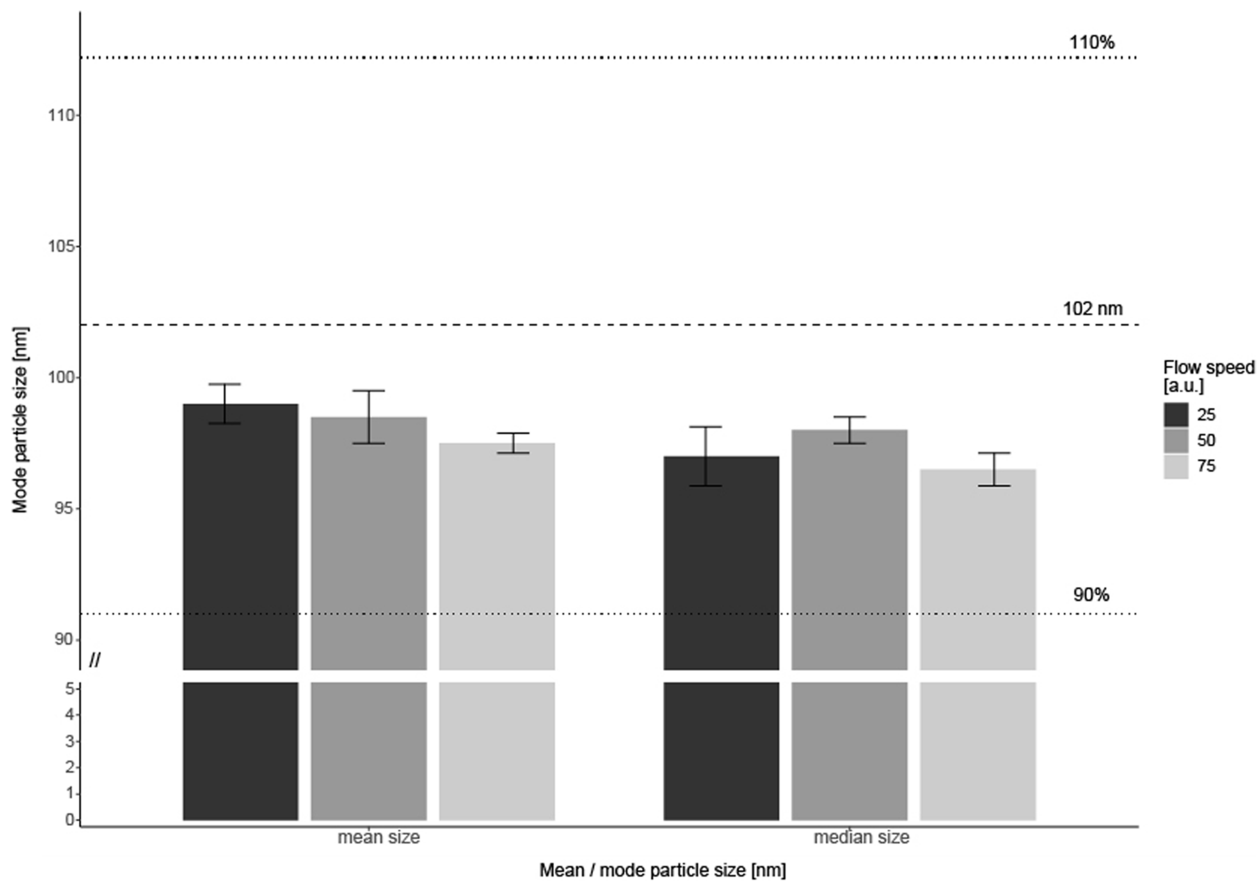

Fig. 7 The influence of flow speed on mean and median particle size expressed in nm as determined for an aqueous suspension of 102 nm Nanospheres analysed in five-fold using CL 11 and DT 15 and with a capturing time of 60 s. Bars indicate ± 1 SD

Table 1 Accuracy, repeatability and within-laboratory reproducibility results with optimised analyses parameters at particle concentrations of 4.0×10^8 and 2.0×10^7 particles/mL

Cell type	Evaluated parameter	Particle concentration [particles/mL]					
		4.0×10^8			2.0×10^7		
		Accuracy [%]	RSD_r [%]	RSD_{RL} [%]	Accuracy [%]	RSD_r [%]	RSD_{RL} [%]
Flow-cell 50 [a.u.]	Particle concentration	84	8.4	15	101	34	37
	Mean size	98	0.8	1.4	102	3.4	5.7
	Mode size	95	1.1	1.2	93	4.6	4.7
O-ring (no flow)	Particle concentration	96	8.6	11	134	47	62
	Mean size	97	1.2	1.3	97	4.5	4.7
	Mode size	95	1.2	1.3	96	6.0	6.4

large differences between individual bottles. This is not unusual and often encountered in the analysis of MPs in bottled water, for instance Oßmann et al. (2018) reported 2689 ± 4371 MP (163%) in bottled water, while Schymanski et al. (2018) reported 118 ± 88 MP (75%) in mineral water of reusable bottles. Comparing the results of this study with other observations is difficult since all other studies were limited to MPs with minimum particle sizes of 1 µm. However, a higher number of particles can be expected when smaller particle sizes are included because of the degradation of larger plastic particles into a higher number of smaller particles. This trend is also clear from

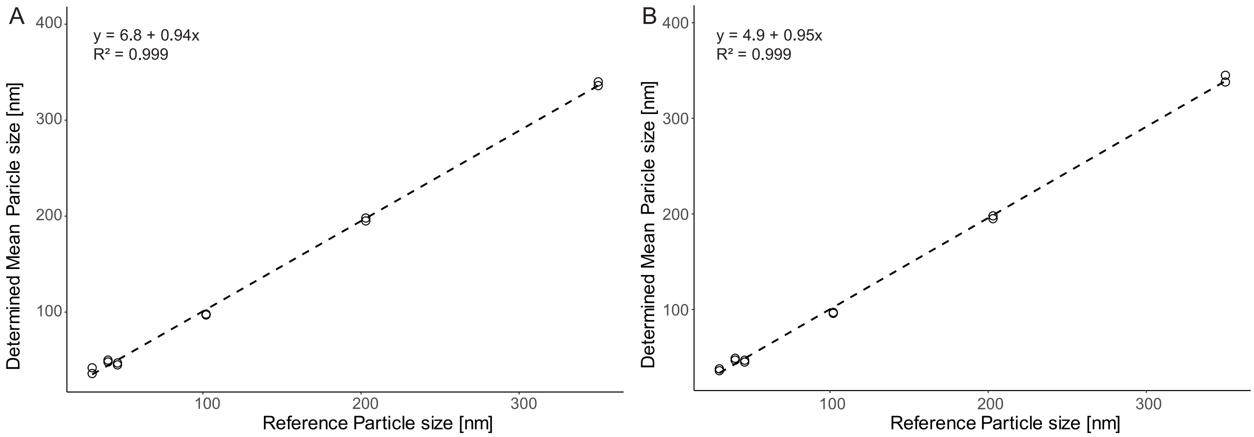

Fig. 8 Calibration curve of the mean (**A**) and mode (**B**) particle size of six standards in the range of 30–350 nm, analysed five-fold. The determined particle size is plotted against the reference particle size

Table 2 Accuracy and repeatability for mean and mode particle size of the calibration standards within a size range of 30–350 nm

Particle size of particle standard [nm]	Mean particle size		Mode particle size	
	Accuracy [%]	RSD_r [%]	Accuracy [%]	RSD_r [%]
30	137	5.3	125	7.4
40	127	5.8	119	2.0
46	103	3.2	95	1.3
102	95	0.6	94	0.8
203	97	1.0	96	1.4
350	96	0.4	97	1.4

the MPs studies that were reported. While Kosuth et al. (2018) report 3.57 particles/L with a smaller particle size of 100 µm, Kankanige et al. (2020) report 140 particles/L with a smaller particle size of 6.5 µm, and Oßmann et al. (2018) report up to 8339 particles/L with a smaller particle size of 1 µm. Zuccarello et al. (2019) even report up to 1.1×10^8 particles/L using a particle size range of 1.28–4.2 µm. So, finding an even higher number of particles in this study may not be surprising. It is also important to note that the NS300 is capable of detecting low-reflecting particles, such as plastic particles, down to approximately 40 nm. However, it is unable to chemically discriminate

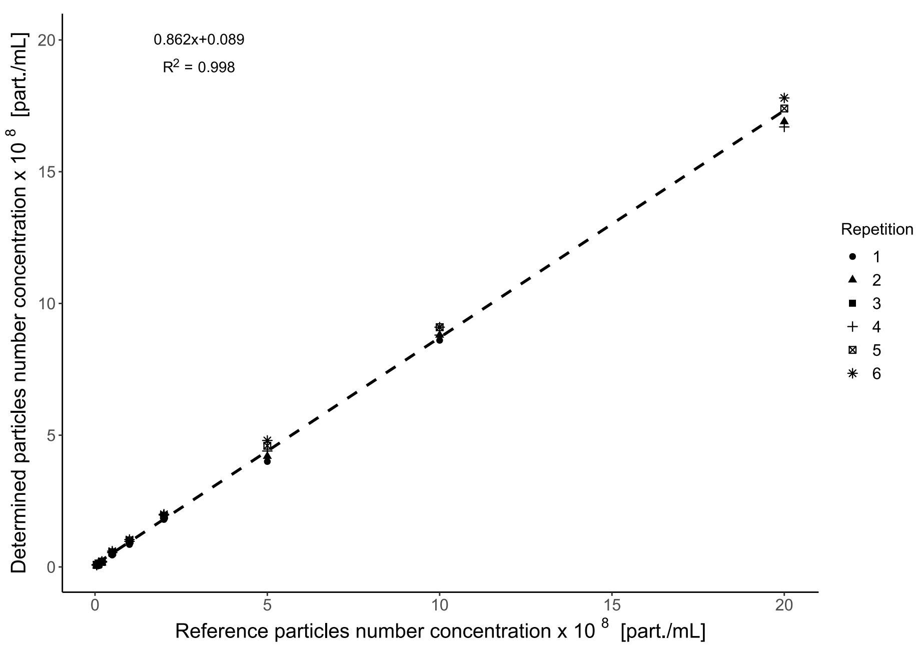

Fig. 9 Calibration curve for 102 nm PS particles with a particle concentration in the range of 5.0×10^6 to 2.0×10^9 part./mL

Table 3 Accuracy and repeatability for 102 nm PS particles with particle concentrations in the range of 5.0×10^6 and 2.0×10^9 part./mL

Particle concentration [part./mL]	Accuracy [%]	RSD_r [%]	$RSD_{criteron.max}$ [%]
2.0×10^9	86	3.2	16
1.0×10^9	89	2.8	18
5.0×10^8	88	9.1	20
2.0×10^8	96	5.2	22
1.0×10^8	97	9.8	25
5.0×10^7	107	14	28
2.0×10^7	91	16	32
1.0×10^7	106	24	35
5.0×10^6	133	36	39

plastic components from non-polymeric particles, which can lead to possible overestimations. Therefore, the obtained results should be further evaluated using alternative methods, such as AFM-IR (Nguyen-Tri et al., 2020), which allow for chemical characterization of the detected particles.

The mean particle size in all bottled water samples is in the range of 110 to 170 nm, while the mode size is between 60 and 90 nm. This means that the most abundant particle size is < 100 nm in all bottled water samples. The higher value for the mean particle size compared to the mode particle size indicates the presence of larger particles. The NS300 can also produce a particle size distribution of an analysed sample. The particle size distribution of the samples A and E are shown in Figs. 10 and 11, respectively.

Conclusions

In the current study, the performance characteristics of NTA for the detection of nanoplastics in water using an NS300 instrument were determined. A camera level of 12 combined with a detection threshold of 14 was determined as an optimal NS300 setting for observing the previously mentioned 102 nm suspension. A capturing time of 60 s combined with a cell flow speed of 50 a.u. showed an acceptable balance between accuracy, precision and analysis time.

The NS300 proved to be accurate and precise for a 102 nm Nanospheres suspension with concentrations of 4.0 $\times 10^8$ and 2.0 $\times 10^7$ particles/mL. The repeatability and reproducibility of the determination of the particle number concentration were 8.4% and 15%, with an accuracy of 84% at the higher concentration. At the lower concentration, the accuracy was 101%, while the repeatability and reproducibility were 34% and 37%, respectively. The concentration range was linear from 5.0×10^6 to 2.0×10^9 particles/mL. For particle size, the instrument's response was linear from 46 to > 350 nm. The accuracy, repeatability and reproducibility for particle size were 95%, 1.1% and 1.2% at a particle number concentration of 4.0×10^8 particles/mL. At the lower concentration of 2.0 $\times 10^7$ particles/mL these numbers were 93%, 4.6% and 4.7%, respectively. From the measurements of mixtures of particles, it can be concluded that NTA has difficulties with polydisperse mixtures, resulting in an underestimation of the smaller particle sizes.

When eight brands of bottled mineral water were analysed, the particle number concentrations ranged from 1.0 $\times 10^6$ to 2.2 $\times 10^7$ particles/mL, with mean

Table 5 Particle number concentrations and particle size (mean and mode) in bottled water samples analysed in ten-fold and with a video capturing time of 180 s

Bottled water samples	Particle number concentration		Particle size	
	Concentration [particles/mL]	RSD_{RL} [%]	Mean [nm]	Mode [nm]
A	1.5×10^7	165	121	75
B	4.0×10^6	45	113	81
C	2.9×10^6	34	163	59
D	1.0×10^6	50	114	85
E	2.2×10^7	13	114	73
F	3.1×10^6	62	119	76
G	2.9×10^6	62	132	91
H	1.3×10^6	72	142	84

Table 4 Accuracy and RSD_r results for particle number concentration and mode particle size of three polydisperse suspensions. Fraction 1 describes the smaller-sized particles, while fraction 2 describes the larger-sized particles

Mixture	Fraction 1				Fraction 2			
	Concentration		Size		Concentration		Size	
	Acc. [%]	RSD_r [%]	Acc. [%]	RSD_r [%]	Acc. [%]	RSD_r [%]	Acc. [%]	RSD_r [%]
46: 102 nm	1.1	105	99	9.7	107	8.4	97	2.5
102: 203 nm	52	10	103	3.1	106	7.1	95	1.9
46: 203 nm	< 1	n.a	n.a	n.a	104	8.4	96	0.7

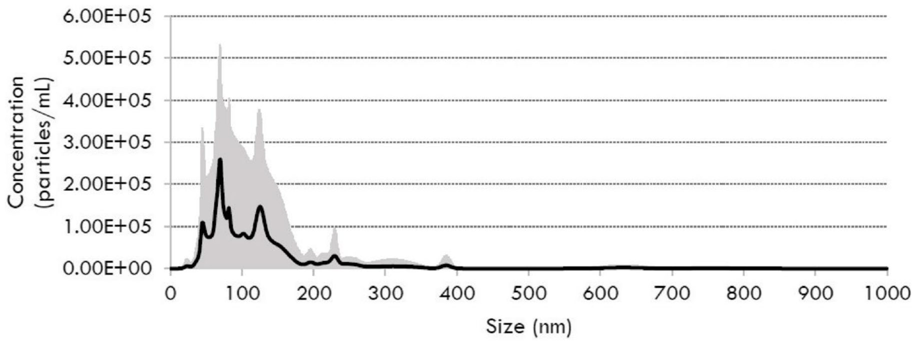

Fig. 10 Averaged particle size distribution (*n* = 10) of brand A bottled water captured with a CL of 16 and video capturing time of 180 s, and processed with a DT of 5. The grey area indicates ± 1 SD

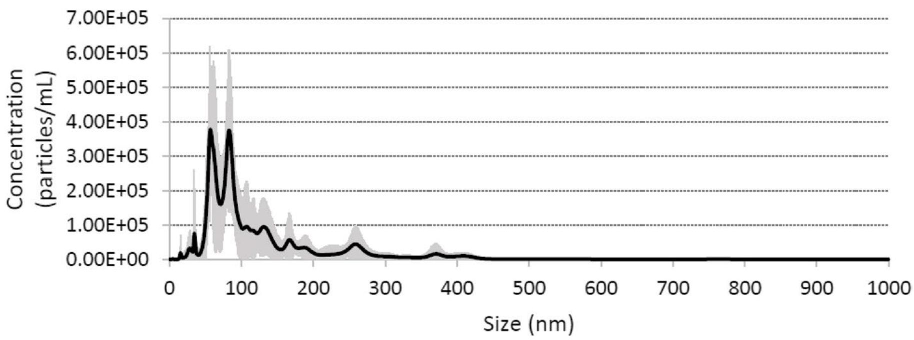

Fig. 11 Averaged particle size distribution (*n* = 10) of brand E bottled water captured with a CL of 16 and video capturing time of 180 s, and processed with a DT of 5. The grey area indicates ± 1 SD

particle sizes in the range of 110 to 170 nm. Since all mode particle sizes were < 100 nm, larger particles are also present. The particle size distributions of two brands of bottled mineral water showed a particle size range of 50 to 500 nm.

Since the NTA technique is unable to recognize or identify plastics, the obtained results reflect the total number of particles, which may include non-plastic particles and lead to an overestimation in bottled water samples. From the results, we conclude that the NTA method is suitable for the detection of monodisperse nanoplastic standards in simple matrices but fails to detect nanoplastics in real world samples due to the inability to distinguish plastics from other reflective particles (e.g., organic matter), resulting in a method prone to overestimation.

Acknowledgements
Not applicable.

Authors' contributions
All the authors contributed significantly to the document and agreed to its publication. RP designed the study. RP and AU drafted the manuscript. ER and ES performed the research and processed the data. All authors read and approved the final manuscript.

Funding
This project has received funding from the European Union's Horizon 2020 Research and Innovation programme under the Grant Agreement number 965367 (PlasticsFatE).

Data availability
Collected and analysed data are available upon request from the corresponding author.

Declarations

Ethics approval and consent to participate
Not applicable.

Consent for publication
All authors give their consent for the publication.

Competing interests
The authors declare no competing interests.

Received: 29 June 2022 Accepted: 19 May 2025
Published online: 30 May 2025

References

Alexy P, Anklam E, Emans T, Furfari A, Galgani F, Hanke G et al (2020) Managing the analytical challenges related to micro- and nanoplastics in the environment and food: filling the knowledge gaps. Food Additives &

Contaminants: Part A. 37(1):1. Available from: (https://www.tandfonline.com/doi/full/10.1080/19440049.2019.1673905) [cited 2022 Jun 23]
Barbosa F, Adeyemi JA, Bocato MZ, Comas A, Campiglia A (2020) A critical viewpoint on current issues, limitations, and future research needs on micro- and nanoplastic studies: From the detection to the toxicological assessment. Environ Res. 182:109089. Available from: (https://linkinghub.elsevier.com/retrieve/pii/S0013935119308850)
Bouwmeester H, Hollman PCH, Peters RJB (2015) Potential Health Impact of Environmentally Released Micro- and Nanoplastics in the Human Food Production Chain: Experiences from Nanotoxicology. Environ Sci Technol. 49(15):8932–47. Available from: (https://pubs.acs.org/doi/10.1021/acs.est.5b01090)
Cai H, Xu EG, Du F, Li R, Liu J, Shi H (2021) Analysis of environmental nanoplastics: Progress and challenges. Chem Eng J. 410:128208. Available from: (https://linkinghub.elsevier.com/retrieve/pii/S1385894720343242)
Caputo F, Vogel R, Savage J, Vella G, Law A, Della Camera G et al (2021) Measuring particle size distribution and mass concentration of nanoplastics and microplastics: addressing some analytical challenges in the sub-micron size range. J Colloid Interfac Sci. 588:401–17. Available from: (https://linkinghub.elsevier.com/retrieve/pii/S0021979720317094)
Dawson AL, Kawaguchi S, King CK, Townsend KA, King R, Huston WM et al (2018) Turning microplastics into nanoplastics through digestive fragmentation by Antarctic krill. Nat Commun. 9(1):1001. Available from: (http://www.nature.com/articles/s41467-018-03465-9)
Ekvall MT, Lundqvist M, Kelpsiene E, Šileikis E, Gunnarsson SB, Cedervall T (2019) Nanoplastics formed during the mechanical breakdown of daily-use polystyrene products. Nanoscale Adv. 1(3):1055–61. Available from: (http://xlink.rsc.org/?DOI=C8NA00210J)
European Commission (2023) Commission Regulation (EU) 2023/2055 of 25 September 2023 amending Annex XVII to Regulation (EC) No 1907/2006 of the European Parliament and of the Council as regards synthetic polymer microparticles. Off J Eur Union. 239:67–104. Available from: (https://eur-lex.europa.eu/eli/reg/2023/2055/oj)
Frias JPGL, Nash R (2019) Microplastics: Finding a consensus on the definition. Marine Pollut Bullet. 138:145–7. Available from: (https://linkinghub.elsevier.com/retrieve/pii/S0025326X18307999)
Gruber ES, Stadlbauer V, Pichler V, Resch-Fauster K, Todorovic A, Meisel TC, Trawoeger S, Hollóczki O, Turner SD, Wadsak W, Vethaak AD, Kenner L (2023) To Waste or Not to Waste: Questioning Potential Health Risks of Micro- and Nanoplastics with a Focus on Their Ingestion and Potential Carcinogenicity. Expo Health. 15(1):33–51. Available from: https://doi.org/10.1007/s12403-022-00470-8
Hartmann NB, Hüffer T, Thompson RC, Hassellöv M, Verschoor A, Daugaard AE et al (2019) Are We Speaking the Same Language? Recommendations for a Definition and sCategorisation Framework for Plastic Debris. Environ Sci Technol. 53(3):1039–47. Available from: (https://pubs.acs.org/doi/10.1021/acs.est.8b05297)
Hernandez LM, Xu EG, Larsson HCE, Tahara R, Maisuria VB, Tufenkji N (2019) Plastic Teabags Release Billions of Microparticles and Nanoparticles into Tea. Environ Sci Technol. 53(21):12300–10. Available from: (https://pubs.acs.org/doi/10.1021/acs.est.9b02540)
Hernandez LM, Yousefi N, Tufenkji N (2017) Are There Nanoplastics in Your Personal Care Products? Environ Sci Technol Lett. 4(7):280–5. Available from: (https://pubs.acs.org/doi/10.1021/acs.estlett.7b00187)
ISO/TR 21960:2020 Plastics — Environmental aspects — State of knowledge and methodologies. Feb, 2020 p. 41. Available from: https://www.iso.org/standard/72300.html
Kankanige D, Babel S (2020) Smaller-sized micro-plastics (MPs) contamination in single-use PET-bottled water in Thailand. Sci Total Environ. 717:137232. Available from: (https://linkinghub.elsevier.com/retrieve/pii/S0048969720307427)
Kestens V, Bozatzidis V, De Temmerman P-J, Ramaye Y, Roebben G (2017) Validation of a particle tracking analysis method for the size determination of nano- and microparticles. J Nanopart Res. 19(8):271. Available from: (http://link.springer.com/10.1007/s11051-017-3966-8)
Kiran BR, Kopperi H, Venkata Mohan S (2022) Micro/nano-plastics occurrence, identification, risk analysis and mitigation: challenges and perspectives. Rev Environ Sci Biotechnol. 21(1):169–203. Available from: (https://link.springer.com/10.1007/s11157-021-09609-6)
Koelmans AA, Besseling E, Foekema EM (2015) Leaching of plastic additives to marine organisms. In: Bergmann M, Gutow L, Klages M (eds) Marine anthropogenic litter. Springer, Cham, pp 199–220. Available from: https://doi.org/10.1007/978-3-319-16510-3_12
Kosuth M, Mason SA, Wattenberg EV (2018) Anthropogenic contamination of tap water, beer, and sea salt. Zhou Z, editor. PLoS ONE. 13(4):e0194970. Available from: (https://dx.plos.org/10.1371/journal.pone.0194970)
Lai H, Liu X, Qu M (2022) Nanoplastics and Human Health: Hazard Identification and Biointerface. Nanomaterials. 12(8):1298. Available from: (https://www.mdpi.com/2079-4991/12/8/1298)
Lambert S, Wagner M (2016) Characterisation of nanoplastics during the degradation of polystyrene. Chemosphere. 145:265–8. Available from: (https://linkinghub.elsevier.com/retrieve/pii/S0045653515304094)
Lambert S, Wagner M (2016) Formation of microscopic particles during the degradation of different polymers. Chemosphere. 161:510–7. Available from: (https://linkinghub.elsevier.com/retrieve/pii/S0045653516309390)
Li D, Shi Y, Yang L, Xiao L, Kehoe DK, Gun'ko YK et al (2020) Microplastic release from the degradation of polypropylene feeding bottles during infant formula preparation. Nat Food. 1(11):746–54. Available from: (https://www.nature.com/articles/s43016-020-00171-y)
Materić D, Kasper-Giebl A, Kau D, Anten M, Greilinger M, Ludewig E et al (2020) Micro- and Nanoplastics in Alpine Snow: A New Method for Chemical Identification and (Semi)Quantification in the Nanogram Range. Environ Sci Technol. 54(4):2353–9. Available from: (https://pubs.acs.org/doi/10.1021/acs.est.9b07540)
Moiniafshari K, Zanut A, Tapparo A, Pastore P, Bogialli S, Abdolahpur MF (2025) A perspective on the potential impact of microplastics and nanoplastics on the human central nervous system. Environ Sci: Nano. 12(3):1809–1820. Available from: (https://pubs.rsc.org/en/content/articlelanding/2025/en/d4en01017e)
Nguyen-Tri P, Ghassemi P, Carriere P, Nanda S, Assadi AA, Nguyen DD (2020) Recent applications of advanced atomic force microscopy in polymer science: A review. Polymers. 12(5):1142. Available from: (https://www.mdpi.com/2073-4360/12/5/1142)
Oelschlägel K, Pfeiffer J, Potthoff A (2018) Imitating the weathering of microplastics in the marine environment. In: Cocca M, Di Pace E, Errico ME, Gentile G, Montarsolo A, Mossotti R, Avella M (eds) Proceedings of the International Conference on Microplastic Pollution in the Mediterranean Sea. Springer, Cham, pp 171–179. Available from: https://doi.org/10.1007/978-3-319-71279-6_23
Oßmann BE, Sarau G, Holtmannspötter H, Pischetsrieder M, Christiansen SH, Dicke W (2018) Small-sized microplastics and pigmented particles in bottled mineral water. Water Res. 141:307–16. Available from: (https://linkinghub.elsevier.com/retrieve/pii/S0043135418303956)
Roesch A, Zölls S, Stadler D, Helbig C, Wuchner K, Kersten G, Hawe A, Jiskoot W, Menzen T (2022) Particles in biopharmaceutical formulations, Part 2: An update on analytical techniques and applications for therapeutic proteins, viruses, vaccines and cells. J Pharm Sci. 111(4):933–950. Available from: https://doi.org/10.1016/j.xphs.2021.12.011
Schymanski D, Goldbeck C, Humpf HU, Fürst P (2018) Analysis of microplastics in water by micro-Raman spectroscopy: Release of plastic particles from different packaging into mineral water. Water Res. 129:154–62. Available from: (https://linkinghub.elsevier.com/retrieve/pii/S0043135417309272)
Singh S, Kumar Naik TSS, Anil AG, Dhiman J, Kumar V, Dhanjal DS et al (2022) Micro (nano) plastics in wastewater: A critical review on toxicity risk assessment, behaviour, environmental impact and challenges. Chemosphere. 290:133169. Available from: (https://linkinghub.elsevier.com/retrieve/pii/S0045653521036419)
Ter Halle A, Jeanneau L, Martignac M, Jardé E, Pedrono B, Brach L et al (2017) Nanoplastic in the North Atlantic Subtropical Gyre. Environ Sci Technol. 51(23):13689–97. Available from: (https://pubs.acs.org/doi/10.1021/acs.est.7b03667)
van Raamsdonk LWD, van der Zande M, Koelmans AA, Hoogenboom RLAP, Peters RJB, Groot MJ et al (2020) Current Insights into Monitoring, Bioaccumulation, and Potential Health Effects of Microplastics Present in the Food Chain. Foods. 9(1):72. Available from: (https://www.mdpi.com/2304-8158/9/1/72)

Vitali C, Peters RJ, Janssen HG, Nielen MW (2022) Microplastics and nanoplastics in food, water, and beverages; part I. Occurrence. TrAC Trends in Analytic Chemi. 159:116670. Available from: (https://linkinghub.elsevier.com/retrieve/pii/S0165993622001534)
Wahl A, Le Juge C, Davranche M, El Hadri H, Grassl B, Reynaud S et al (2021) Nanoplastic occurrence in a soil amended with plastic debris. Chemosphere. 262:127784. Available from: (https://linkinghub.elsevier.com/retrieve/pii/S0045653520319792)
Zhang Q, Xu EG, Li J, Chen Q, Ma L, Zeng EY et al (2020) A Review of Microplastics in Table Salt, Drinking water, and Air: Direct Human Exposure. Environ Sci Technol. 54(7):3740–51. Available from: (https://pubs.acs.org/doi/10.1021/acs.est.9b04535)
Zuccarello P, Ferrante M, Cristaldi A, Copat C, Grasso A, Sangregorio D et al (2019) Exposure to microplastics (<10 µm) associated to plastic bottles mineral water consumption: The first quantitative study. Water Res. 157:365–71. Available from: (https://linkinghub.elsevier.com/retrieve/pii/S0043135419302921)

Publisher's Note